AIChE

Prediction of TMCH Thermal Hazard with Various Calorimetric Tests by Green Thermal Analysis Technology

Jo-Ming Tseng and Jian-Zhi Lin
Institute of Safety and Disaster Prevention Technology, Central Taiwan University of Science and Technology,
Beitun District, Taichung, Taiwan 40601, R.O. China

Chuan-Chen Lee and Chun-Ping Lin
Dept. of Health and Nutrition Biotechnology, College of Health Science, Asia University, Wufeng, Taichung, Taiwan
41354, R.O. China

DOI 10.1002/aic.13745

*1,1,-Di-(*tert*-butylperoxy)-3,3,5-trimethylcyclohexane (TMCH), a liquid organic peroxide, has been widely used in the chemical industry as a polymerization initiator. The thermokinetic parameters of TMCH are investigated by three types of calorimetric tests (isothermal, nonisothermal, and adiabatic) to determine thermal decomposition properties of TMCH using differential scanning calorimetry (DSC) isothermal tests, DSC nonisothermal tests, and vent sizing package 2 adiabatic tests, respectively. Comparisons of three kinds of thermal analysis models were done for kinetics simulation, which can result in a beneficial kinetic model and parameters of thermal decomposition of TMCH. The use of green technology to replace the complex methods and energy consumption of the traditional self-accelerating decomposition temperature tests are discussed. There are significant disadvantages with traditional thermal analysis methods in terms of a novel, swift, and green technology, which is the achieved object here for preventing pollution and reducing energy consumption.* © 2012 American Institute of Chemical Engineers *AIChE J,* 58: 3792–3798, 2012

Keywords: organic peroxide, differential scanning calorimetry, vent sizing package 2, kinetic model, green technology

Introduction

This aim of the study was to use isothermal, nonisothermal, and adiabatic tests of kinetics to predict the thermal decomposition mechanism of a liquid organic peroxide, such as 1,1,-di-(*tert*-butylperoxy)-3,3,5-trimethylcyclohexane (TMCH). TMCH, like many organic peroxides, should follow the United Nations (UN) "recommendations on the transport of dangerous goods" and the "European agreement concerning the international carriage of dangerous goods" for the safety management of reactive substances during storage and transportation.[1–4] The goal of this study was to develop a beneficial kinetic model and reliable thermokinetic parameters of thermal decomposition of TMCH and then processing liquid explosion simulation.

Differential scanning calorimetry (DSC) was simply used to assess the isothermal and nonisothermal kinetics. DSC is a popular and practical thermal analyzer, which can be applied on the thermal analysis in widespread chemicals or materials. Actually, following famous scientists, such as Kissinger, Ozawa, Augis, and Bennett, we only acquired limited thermokinetic parameters via their well-known kinetic equations.[5–10] Unfortunately, the results of thermokinetic parameters did not satisfy application during process, storage, and transportation safety.

Therefore, using DSC isothermal tests, DSC nonisothermal tests, and vent sizing package 2 (VSP2) adiabatic tests, respectively, we then compared the thermokinetic parameters of TMCH to determine the properties of thermal decomposition. Kinetic simulation was used to construct a precise and effective procedure to evaluate the thermokinetic parameters for the thermal decomposition of TMCH.[11–14] The chosen approach was to obtain the beneficial kinetics and reliable parameters of the thermal decomposition that included the kinetic parameters and inherently safe properties, such as the mechanism of thermal decomposition, heat of decomposition (ΔH_d), reaction order (n), activation energy (E_a), isothermal time to maximum rate ($\mathrm{TMR_{iso}}$), and time to conversion limit (TCL).

The self-accelerating decomposition temperature (SADT) is generally determined by one of four testing methods recommended in the UN orange book: the United States (US) SADT test, the adiabatic storage test, the isothermal storage test, and the heat accumulation storage test.[14,15] First, this study developed a suitable kinetic model and adequate thermokinetic parameters of thermal decomposition of TMCH, which could be applied to liquid explosion simulation. The intent was to develop a simple and swift simulated method that could replace the inaccurate computations by the traditional SADT test.[16] The chosen approach was to establish an efficient procedure for the thermal hazard assessment that included the safety parameters, such as the SADT, control temperature (CT), emergency temperature (ET), and the

---

Correspondence concerning this article should be addressed to C.-P. Lin at chunping927@gmail.com.

Table 1. Results for the Thermal Decompositions of TMCH from the DSC Isothermal Tests

Sample Mass (mg)	Isothermal Conditions (°C)	ΔH_d (kJ kg^{-1})
3.1	115	833
3.2	120	962
3.0	125	983
3.2	130	1042

critical temperature (TCR), for a container or reactor containing TMCH. There are significant disadvantages with these four methods in terms of novel, swift, and green thermal analysis technology, which is based on preventing pollution and reducing energy consumption.

Application of Green Thermal Analysis Technology

Kinetic model simulation

Simulations of kinetic models can be complex multistage reactions with several independent, parallel, and consecutive stages[10–14]:

- Simple single-stage reaction

$$\frac{d\alpha}{dt} = k_0 e^{\frac{-E_a}{RT}} f(\alpha) \tag{1}$$

- Single-stage for *n*th order reaction

$$\frac{d\alpha}{dt} = k_0 e^{\frac{-E_a}{RT}} (1-\alpha)^n \tag{2}$$

- Multistage for autocatalytic reaction

$$f(\alpha) = (1-\alpha)^{n_1}(\alpha^{n_2} + z) \tag{3}$$

where E_a is the activation energy, k_0 is the pre-exponential factor, z is the autocatalytic constant, and n_1 and n_2 are the reaction orders of a specific stage.

Reactions that include two consecutive stages are as follows[10–14]

$$\frac{d\alpha}{dt} = k_1 e^{\frac{-E_1}{RT}} (1-\alpha)^{n_1};\ \frac{d\gamma}{dt} = k_2 e^{\frac{-E_2}{RT}} (\alpha-\gamma)^{n_2} \tag{4}$$

where α and γ are the conversions of the reactant A and product C, respectively. E_1 and E_2 are the activation energies of the stages.[10–14]

Two parallel reactions for full autocatalysis are as follows

$$\frac{d\alpha}{dt} = r_1(\alpha) + r_2(\alpha); \quad \begin{array}{l} r_1(\alpha) = k_1(T)(1-\alpha)^{n_1} \\ r_2(\alpha) = k_2(T)\alpha^{n_2}(1-\alpha)^{n_3} \end{array} \tag{5}$$

where r_1 and r_2 are the rates of each stage, and n_3 is the reaction order of stage 3.

Table 2. Results for the Thermal Decompositions of TMCH from the DSC Nonisothermal Tests

Sample Mass (mg)	Scanning Rate (°C min^{-1})	Onset Temperature, T_o (°C)	Peak of Temperature, T_p (°C)	ΔH_d (kJ kg^{-1})
2.9	1	106	131	1151
2.9	2	115	138	1056
3.0	4	122	144	1020
3.0	6	123	149	1370

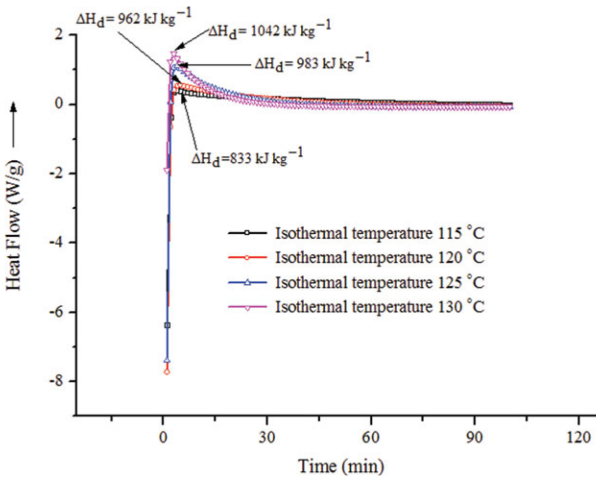

Figure 1. Isothermal curves for TMCH decomposition with DSC isothermal tests under 115, 120, 125, and 130°C.

[Color figure can be viewed in the online issue, which is available at wileyonlinelibrary.com.]

Thermal hazard simulations

To simulate the thermal hazard of liquid organic peroxide, the critical parameters for the thermal hazard were determined numerically from the chemical kinetics for several types of reactor geometries and various boundary conditions, including the possibility of setting boundary shells. For liquid thermal hazard simulations, the following statements were used[13,14]

$$\rho C_P \frac{\partial T}{\partial t} = \mathrm{div}(\lambda \Delta T) + W \qquad \text{Thermal conductivity equation} \tag{6}$$

$$\frac{\partial \alpha_i}{\partial t} = r_i \ i = 1, \ldots \mathrm{NC} \qquad \text{Kinetic equations (formal models)} \tag{7}$$

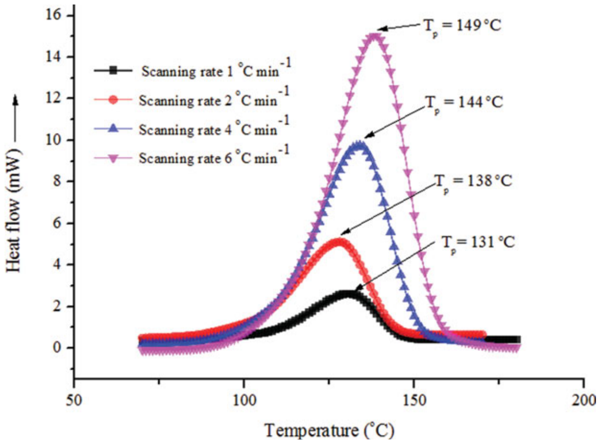

Figure 2. Nonisothermal curves for TMCH decomposition with DSC nonisothermal tests of scanning rates at 1, 2, 4, and 6°C min^{-1}.

[Color figure can be viewed in the online issue, which is available at wileyonlinelibrary.com.]

Table 3. Results for the Thermal Runaway Reaction of TMCH by VSP2 Tests with Various Concentrations

Sample	T_{max} (°C)	P_{max} (bar)	$(dP\ dt^{-1})_{max}$ (bar min^{-1})	$(dT\ dt^{-1})_{max}$ (°C min^{-1})
TMCH (10 mass %, 20 mL)	227.48	10.81	21.81	345.49
TMCH (20 mass %, 20 mL)	229.87	11.65	883.94	4862.40
TMCH (25 mass %, 20 mL)	254.71	14.11	915.25	7086.78

$$W = \sum_{(i)} Q_i^{\infty} r_i \qquad \text{Heat power equation} \qquad (8)$$

where T is the temperature, t is the time, ρ is the density, C_P is the specific heat, λ is the heat conductivity, Q_i^{∞} is the reaction calorific effect, W is the heat power, r is the reaction rate constant, α is the degree of conversion for a component, NC is the number of components, and i is the component number.

The initial fields for the temperature and the conversions were constant throughout the reactor volume[13,14]

$$\begin{aligned} T|_{t=0} &= T_0 \\ \alpha_i|_{t=0} &= \alpha_{i0} \end{aligned} \qquad (9)$$

The index 0 indicates the initial values of the temperature and conversion.

The boundary conditions of the first, second, and third kind were specified as follows[13,14]

$$\text{First kind}: \ T|_{\text{wall}} = T_e(t) \qquad \text{Temperature} \qquad (10)$$

$$\text{Second kind}: \ q|_{\text{wall}} = q(t) \qquad \text{Heat flow} \qquad (11)$$

$$\text{Third kind}: -\lambda \left.\frac{\partial T}{\partial n}\right|_S = \chi(T_{\text{wall}} - T_e) \qquad \text{Newton's cooling law} \qquad (12)$$

The indices "wall" and "e" relate to the parameters on the boundary and the environment, respectively; q is the heat flow, and n is the unit outer normal on the boundary.

Experimental Method

Samples

TMCH, 88 mass %, which was purchased directly from ACE Chemical Corp in Taiwan, was stored in a refrigerator at 4°C. To avoid bursting the test cell and losing all of the exothermic data, the VSP2 tests were run with 10–25 mass %.

Differential scanning calorimetry

Temperature-programmed screening experiments were performed with DSC (TA Q20). The test cell was used to carry out the experiment for withstanding the relatively high pressure to ~10 MPa. ASTM E698 was used to obtain thermal curves for calculating kinetic parameters. Approximately 2–3 mg of the sample was used to acquire the experimental data. Nonisothermal tests of the scanning rate selected for the programmed temperature ramp were 1, 2, 4, and 6°C min^{-1}. The range of temperature rise chosen was from 30 to 300°C for each experiment. Isothermal tests of the holding isothermal condition were at 115, 120, 125, and 130°C for TMCH. The results for the thermal decompositions of TMCH from the isothermal and nonisothermal of DSC tests are listed in Tables 1 and 2, and the test curves of DSC are shown in Figures 1 and 2, respectively.

Vent sizing package 2

VSP2, developed by Fauske and Associates,[17] is a highly sensitive calorimeter that can obtain thermokinetic and thermal decomposition data, such as temperature and pressure traces with respect to time in an adiabatic calorimeter system by PC control. Under heating conditions, the main heater heats the sample to a preset temperature and then a guard heater maintains an adiabatic environment. In the experimental conditions, if the self-heating rate is larger than 0.02°C min^{-1}, the heat-wait-search stage and main heater should be immediately stopped for measuring the original phenomenon of self-exothermicity. To adequately protect the normal operation of this apparatus and avoid bursting the test cell and missing the end of exothermic data, the 15, 20, and 25 mass % of TMCH were prudently chosen for the experiments. Thermokinetic and pressure behavior in the same test cell (112 mL)

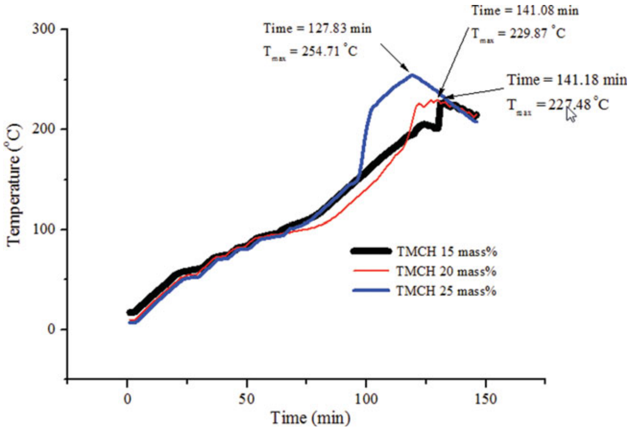

Figure 3. Temperature vs. time for thermal runaway reaction of TMCH with various concentrations by VSP2.

[Color figure can be viewed in the online issue, which is available at wileyonlinelibrary.com.]

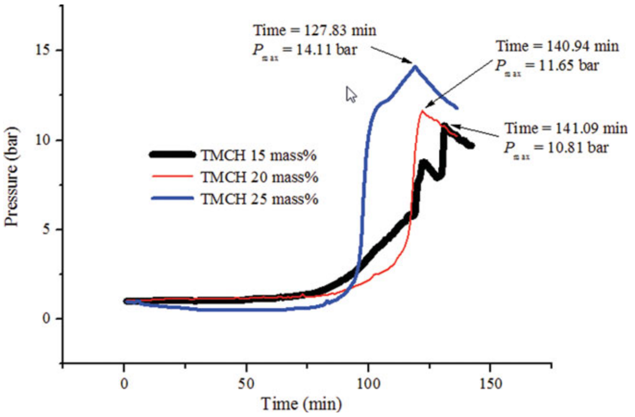

Figure 4. Pressure vs. time for thermal runaway reaction of TMCH with various concentrations by VSP2.

[Color figure can be viewed in the online issue, which is available at wileyonlinelibrary.com.]

Table 4. The Reactor Size and Boundary Conditions for the 0.5 L Vessel, 25 kg Barrel Package by Simulation

Package Size	Radius (m)	Height (m)	Shell Thickness (m)	Boundary Conditions	χ (W m^{-2} K^{-1})
0.5 L	0.0286	0.18	0.00286	Top/3rd kind, Side/3rd kind, Bottom/1st kind	10/10/–
25 kg	0.20	0.3	0.015	Top/3rd kind, Side/3rd kind, Bottom/1st kind	10/10/–

Table 5. The Thermokinetic Parameters Evaluated by Isothermal Kinetic Simulation

	Isothermal Temperature (°C)							
	115		120		125		130	
Kinetic Model	*N*th Order	Autocatalytic	*N*th Order	Autocatalytic	*N*th Order	Autocatalytic	*N*th Order	Autocatalytic
ln(k_0)/ln (s^{-1})	8.5621	36.3358	30.1986	34.7442	36.0592	35.7997	63.2576	34.3089
E_a (kJ mol^{-1})	54.9063	143.0949	130.4274	143.5340	144.5241	141.9140	235.3652	142.1635
Reaction order (n)/nth Reaction order (n_1)/auto	$1.000E-08$	0.8541	0.9065	1.1099	0.1260	1.0024	0.2900	1.7686
Reaction order (n_2)	N/A	0.7530	N/A	0.2063	N/A	0.9546	N/A	0.5947
Autocatalytic constant (z)	N/A	$5.259E-04$	N/A	$4.578E-03$	N/A	$1.095E-03$	N/A	$8.392E-04$
ΔE$_d$ (kJ kg^{-1})	149.2444	898.2610	744.1244	587.5223	259.8419	758.0646	265.3337	802.7405

N/A, not available

Table 6. The Thermokinetic Parameters Evaluated by Nonisothermal Kinetic Simulation

	Scanning Rate (°C min^{-1})							
	1		2		4		6	
Kinetic Model	*N*th Order	Autocatalytic	*N*th Order	Autocatalytic	*N*th Order	Autocatalytic	*N*th Order	Autocatalytic
ln(k_0)/ln (s^{-1})	10.4633	36.3035	34.2247	35.9946	23.2783	36.0124	12.2532	36.1150
E_a (kJ mol^{-1})	59.8382	143.0720	136.4269	143.0190	99.7319	144.2466	62.6662	142.5152
Reaction order (n)/nth Reaction order (n_1)/auto	0.1276	1.0533	0.9912	1.0696	0.5870	1.1542	0.1631	1.4479
Reaction order (n_2)	N/A	$3.048E-08$	N/A	$3.000E-08$	N/A	0.0292	N/A	0.2432
Autocatalytic constant (z)	N/A	0.0208	N/A	0.2541	N/A	0.9323	N/A	0.1596
ΔE$_d$ (kJ kg^{-1})	1182.6902	1163.0723	1229.6047	1229.4272	1313.1772	1295.2045	1386.9342	1383.6773

N/A, not available

usually could be tested without any difficult extrapolation to the process scale due to the low thermal inertia factor (Φ) of about 1.05–1.32.[17] The low Φ allows for bench-scale simulation of the worst credible case, such as wrong dosing, cooling failure, or external fire conditions. The results for the adiabatic runaway reaction of TMCH from the 15, 20, and 25 mass % of VSP2 tests are listed in Table 3.

Figure 3 shows the temperature vs. time for thermal decomposition of 15, 20, and 25 mass % TMCH by VSP2. Meanwhile, pressure vs. time by VSP2 under various concentrations is shown in Figure 4. For 25 mass %, as in Figure 3, $T_{\max}$ reached 254.71°C and as in Figure 4, $P_{\max}$ reached 14.11 bar. The $(dT\ dt^{-1})_{\max}$ and $(dP\ dt^{-1})_{\max}$ of 25 mass % were about 7086.78°C min^{-1} and 915.25 bar min^{-1}, respectively, as revealed in Table 3.

Liquid thermal explosion simulation

This study used a 0.5 L Dewar vessel for matching US SADT test and a 25 kg barrel container for commercial package as the reactor sizes to simulate the thermal hazard. The radius, height, and shell thickness and the reactors boundary conditions are listed in Table 4.

Results and Discussion

Determination of thermokinetic parameters by kinetic model simulation

The kinetic parameters were determined from the DSC experimental data at various scanning rates of 1, 2, 4, and 6°C min^{-1}, isothermal tests holding isothermal conditions of 115–130°C, and adiabatic runaway reaction of 15, 20, and

Table 7. The Thermokinetic Parameters Evaluated by Adiabatic Kinetic Simulation

	Sample (mass %)					
	15		20		25	
Kinetic Model	*N*th Order	Autocatalytic	*N*th Order	Autocatalytic	*N*th Order	Autocatalytic
ln(k_0)/ln (s^{-1})	36.5461	39.6004	13.4316	38.4507	42.9170	39.9958
E_a (kJ mol^{-1})	108.5819	97.1031	50.4873	99.9636	120.7261	100.0155
Reaction order (n)/nth Reaction order (n_1)/auto	1.0352	1.0079	0.9119	1.7903	0.9017	1.3147
Reaction order (n_2)	N/A	1.1609	N/A	0.4080	N/A	0.9485
Autocatalytic constant (z)	N/A	0.0113	N/A	0.0261	N/A	0.0118
ΔE$_d$ (kJ kg^{-1})	113.9704	105.5058	108.9312	100.6469	92.8884	84.1220

N/A, not available

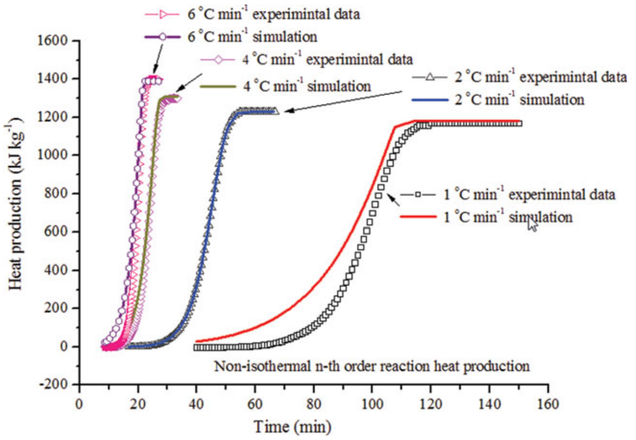

Figure 5. TMCH heat production vs. time curves of the *n*th order reaction with scanning rates of 1, 2, 4, and 6°C min^{-1} by experiment and simulation.

[Color figure can be viewed in the online issue, which is available at wileyonlinelibrary.com.]

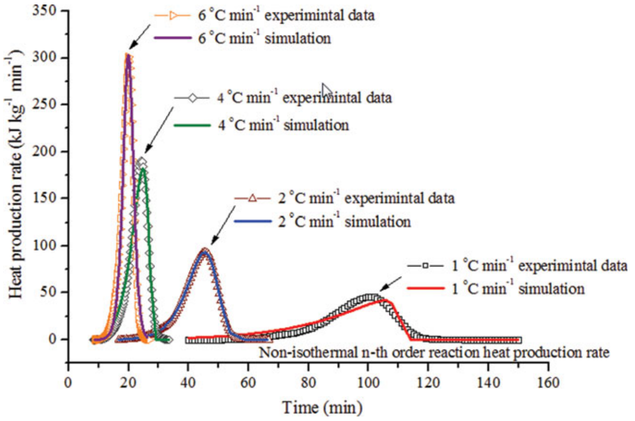

Figure 7. TMCH heat production rate vs. time curves of the autocatalytic reaction with scanning rates of 1, 2, 4, and 6°C min^{-1} by experiment and simulation.

[Color figure can be viewed in the online issue, which is available at wileyonlinelibrary.com.]

25 mass % of VSP2 tests for TMCH. The thermal decomposition of TMCH represents an unknown mechanism of reaction, such as an *n*th order or autocatalytic reaction. Here, using the *n*th order and autocatalytic simulations to calculate the thermokinetic parameters and then to compare the results of isothermal, nonisothermal, and adiabatic of kinetic model simulation, we obtained the beneficial mechanism of thermal decomposition for TMCH. The simulation results are presented in Tables 5–7.

From comparisons of isothermal, nonisothermal, and adiabatic kinetic model, *n*th order reaction, and autocatalytic reaction, we obtained better results for the thermal hazard parameters of thermal decomposition. Despite the fact that the use of simulated *n*th order and autocatalytic reaction kinetics to match original DSC experimental data (Tables 1 and 2) was proven to give superior results, not all of the data are compatible with the model. In addition, from comparisons of thermokinetic parameters of isothermal, nonisothermal, and adiabatic kinetic model simulation, and the kinetic parameters of TMCH, the mechanism of thermal decomposition belongs to the autocatalytic reaction.

Tables 5 and 6 show that they can be matched well to the results of the autocatalytic simulations for TMCH. Comparison of Tables 5 and 6 shows that the samples were tested under the high isothermal conditions; to compare, the overheating effect was greater than nonisothermal DSC tests. Thus, the result of isothermal-kinetic-model simulation was concerned with the overheating effect of the kinetic parameters and they were excluded from further analysis.

Table 7 shows the results of the adiabatic runaway reaction kinetic simulation of TMCH. However, this study used a low concentration of TMCH solution as 15, 20, and 25 mass %, which cannot do what on behalf of the original sample. Thus, from the result of adiabatic kinetic simulation, the data set was also excluded from further analysis. Fortunately, from Table 7 we can observe the mechanism of thermal decomposition, which tends to an autocatalytic reaction for adiabatic kinetic simulation. Therefore, this study

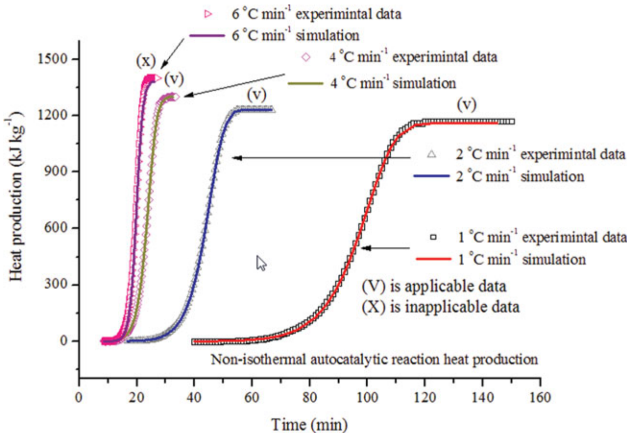

Figure 6. TMCH heat production vs. time curves of the autocatalytic reaction with scanning rates of 1, 2, 4, and 6°C min^{-1} by experiment and simulation.

[Color figure can be viewed in the online issue, which is available at wileyonlinelibrary.com.]

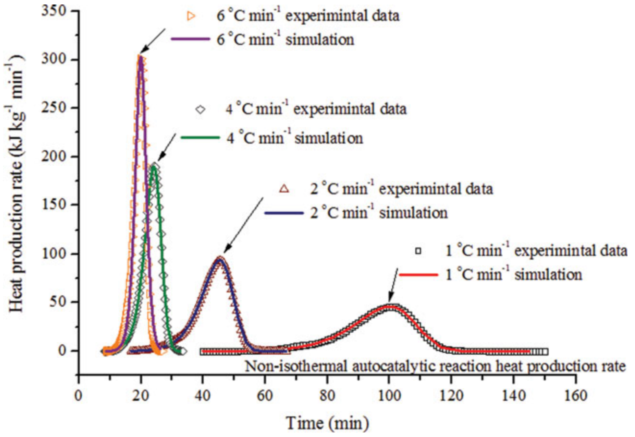

Figure 8. TMCH heat production rate vs. time curves of the autocatalytic reaction with scanning rates of 1, 2, 4, and 6°C min^{-1} by experiment and simulation.

[Color figure can be viewed in the online issue, which is available at wileyonlinelibrary.com.]

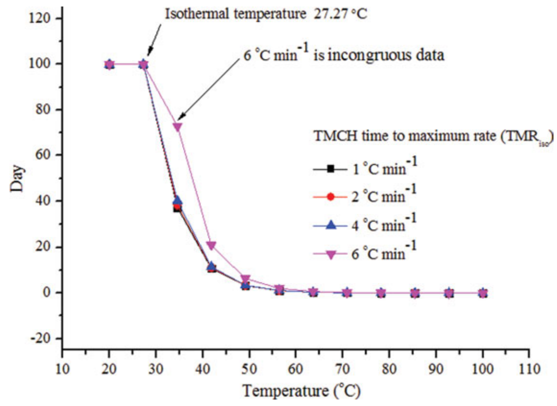

Figure 9. Simulated TMCH time until the maximum rate was achieved with nonisothermal autocatalytic kinetic simulation.

[Color figure can be viewed in the online issue, which is available at wileyonlinelibrary.com.]

demonstrated the "beneficial kinetic" for thermal decomposition of TMCH. Now, a more important matter is to find the "reliable thermokinetic parameters" from the nonisothermal autocatalytic simulation.

Comparisons of experimental data and data derived from simulated *n*th order reaction and autocatalytic reaction for heat production and heat production rate vs. time are shown in Figures 5–8, respectively. Here too, despite the fact that the use of simulated autocatalytic kinetic models to match original DSC experimental data (from Figures 5 to 8) was proven to give superior results, not all of the data are compatible with the model.

The TMR$_{iso}$, TER, and TCL of TMCH were acquired by simulating autocatalytic nonisothermal simulation, as displayed in Figures 9–11. Figure 9 shows the TMR$_{iso}$ of TMCH obtained, in which the values were below 27.27°C and exceeded the upper 100 days, and Figure 10 shows that the TER of TMCH is stored below 27.27°C, which is safe. Figure 11 shows that the TCL of TMCH is below 20°C, which is beyond the upper limit of 10 years. All of the inherently safe parameters of thermal decomposition were acquired by nonisothermal autocatalytic kinetic model simulation.

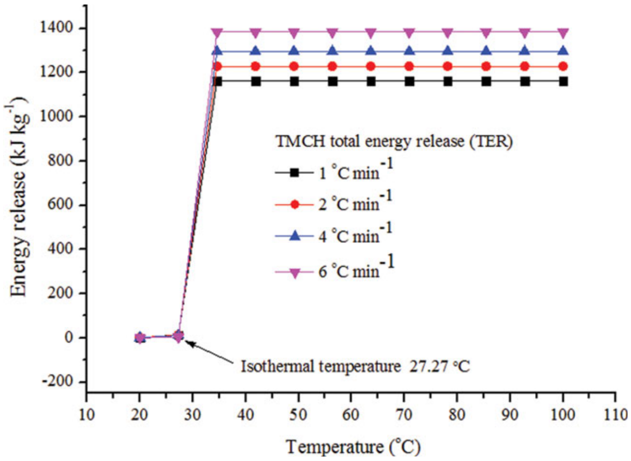

Figure 10. Simulated TMCH total energy release with nonisothermal autocatalytic kinetic simulation.

[Color figure can be viewed in the online issue, which is available at wileyonlinelibrary.com.]

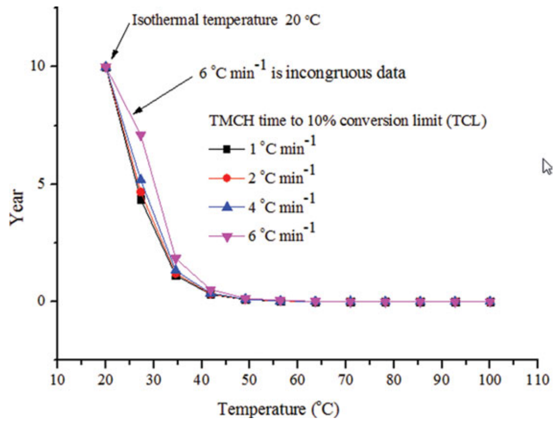

Figure 11. Simulated TMCH time until 10% conversion of the thermal decomposition was achieved with nonisothermal autocatalytic kinetic simulation.

[Color figure can be viewed in the online issue, which is available at wileyonlinelibrary.com.]

In Figures 6 and 9–11, the heat effect of TMCH at the 6°C min^{-1} scanning rate is greater than that observed at the other scanning rates. While analyzing the thermokinetic parameters by kinetic model simulation, we obtained three values for the autocatalytic thermokinetic parameters by using scanning rates of 1, 2, and 4°C min^{-1} in the thermal hazard simulation. This data set was excluded from further analysis.

Now, we have obtained the "reliable thermokinetic parameters" from the aforementioned analysis. The analysis of thermokinetic parameters of the thermal decomposition of TMCH depends on the reliability of the kinetic model.

Dewar vessel and 25 kg barrel package thermal hazard simulations

The results of the thermal hazard simulation for the SADT, CT, ET, and TCR are presented in Table 8. The thermal decomposition stability of 0.5 L Dewar vessels was greater than that of the 25 kg package. The stability and applicability worsened as the reactor size increased. The results of thermal hazard assessment also proved that the smaller size container has a better beneficial exothermal effect for containment of organic peroxide than a huge package.

These results could be applied toward energy reduction and safer designs for use and in storage.

In addition to analyze the thermal decomposition kinetic parameters through comparing isothermal, nonisothermal, and adiabatic-kinetic model simulations, we found that the results

Table 8. A Comparison of the Values from the Literature and the Liquid Thermal Explosion Simulation for the SADT, CT, ET, and TCR at Scanning Rates of 1, 2, and 4°C min^{-1} in the 0.5 L Vessel, and 25 kg Package

Size	Scanning Rate	SADT (°C) in Literature	SADT (°C)	CT (°C)	ET (°C)	TCR (°C)
0.5 L	1	60*, >60[†], 65[‡]	76	66	71	76.63
	2		77	67	72	75.69
	4		76	66	71	76.01
25 kg	1		65	55	60	63.74
	2		65	55	60	63.80
	4		65	55	60	63.73

*Akzo Nobel 25 kg package.[3]
[†]Pergan GmbH 25 kg package.[4]
[‡]Bosch et al. experimental value.[16]

presented a beneficial kinetic model and reliable thermokinetic parameters of thermal decomposition. The model can be applied to evaluate other organic peroxides or chemicals.

Conclusions

This study applied the isothermal, nonisothermal, and adiabatic kinetic models for the evaluation of thermokinetic parameters and compared the results to simulated thermal analysis. This approach led to the development of an effective, precise procedure for the evaluation of a beneficial kinetic model and reliable thermokinetic parameters of TMCH.

Comparisons of isothermal, nonisothermal, and adiabatic calorimetric tests provided precise kinetic information depending on available thermal analysis technology. We have shown that through green thermal analysis technology one can determine a beneficial kinetic model and reliable thermokinetic parameters, which can swiftly and effectively predict the thermal hazard of TMCH.

We also obtained amazing results for predicting thermal hazard using only isothermal and nonisothermal calorimetric analysis, which could satisfy our research for evaluating the safety parameters of TMCH. There are significant disadvantages with traditional thermal analysis methods in terms of a novel, swift, and green technology, which is the achieved objective for preventing pollution and reducing energy consumption.

Acknowledgments

The authors are indebted to the donors of the National Science Council (NSC) in Taiwan under the contract number NSC 100-2218-E-468-001- for financial support. They are grateful to ACE Chemical Corp. in Taiwan, ROC. In addition, they are indebted to Prof. Chi-Min Shu for technical support on the VSP2 experiments.

Notation

C_P = specific heat capacity, J g^{-1} K^{-1}
CT = control temperature, °C
DSC = differential scanning calorimetry
E_a = activation energy, kJ mol^{-1}
E_1 = activation energy of the first stage, kJ mol^{-1}
E_2 = activation energy of the second stage, kJ mol^{-1}
ET = emergency temperature, °C
f_i = kinetic functions of the *i*th stage, $i = 1, 2, 3$
$f(\alpha)$ = kinetic functions
k_0 = pre-exponential factor, m^3 mol^{-1} sec^{-1}
k_i = reaction rate constant, $i = 1, 2$, mol L^{-1} sec^{-1}
N/A = not available
n = reaction order or unit outer normal on the boundary, dimensionless
NC = number of components, dimensionless
n_i = reaction order of the *i*th stage, $i = 1, 2, 3$, dimensionless
$P_{\max}$ = maximum explosion pressure, bar
Q_i^{∞} = specific heat effect of a reaction, J kg^{-1}
q = heat flow, J g^{-1}
r_i = reaction rate of the *i*th stage, $i = 1, 2, 3, 4$, g sec^{-1}
S = heat-exchange surface, m^2
SADT = self-accelerating decomposition temperature, °C
T = absolute temperature, K
T_0 = exothermic onset temperature, °C
TCL = time to conversion limit, year
TCR = critical temperature, °C
TER = total energy release, kJ kg^{-1}
T_e = ambient temperature, °C
$T_{\max}$ = maximum explosion pressure, °C
TMCH = 1,1,-di-(*tert*-butylperoxy)-3,3,5-trimethylcyclohexane
$\mathrm{TMR_{iso}}$ = time to maximum rate under isothermal conditions, day
T_p = peak temperature, °C
T_{wall} = temperature on the wall, °C
t = time, s
VSP2 = vent sizing package 2
W = heat power, W g^{-1}
z = autocatalytic constant, dimensionless
$(dP\ dt^{-1})_{\max}$ = maximum rate of explosion pressure rise, bar min^{-1}
$(dT\ dt^{-1})_{\max}$ = maximum rate of explosion temperature rise, °C min^{-1}

Greek letters

α = degree of conversion, dimensionless
α_i = degree of conversion of the *i*th stage, $i = 1, 2, 3, 4$, dimensionless
γ = degree of conversion, dimensionless
ρ = density, kg m^{-3}
λ = heat conductivity, W m^{-1} K^{-1}
χ = heat-transfer coefficient, W m^{-2} K^{-1}
ΔH_d = heat of decomposition, kJ kg^{-1}
Φ = thermal inertia factor, dimensionless

Literature Cited

1. United Nations. *Recommendations on the Transport of Dangerous Goods, Model Regulations*, 16th rev. ed. New York: United Nations, 2009.
2. United Nations. *European Agreement Concerning the International Carriage of Dangerous Goods by Road (ADR)*. New York: United Nations, 2009.
3. Akzo Nobel Polymer Chemicals. *Production Data Sheet*. Deventer, The Netherlands: Akzo Nobel Polymer Chemicals, 2008.
4. PERGAN GmbH. *Material Safety Data Sheet*. Bocholt, Germany: PERGAN GmbH, 2011.
5. Vyazovkina S, Burnhamb AK, Criadoc JM, Pérez-Maquedac LA, Popescud C, Sbirrazzuolie N. Review ICTAC Kinetics Committee recommendations for performing kinetic computations on thermal analysis data. *Thermochim Acta*. 2011;520:1–19.
6. Kissinger HE. Reaction kinetics in differential thermal analysis. *Anal Chem*. 1957;29:1702–1706.
7. Ozawa T. Estimation of activation energy by isoconversion methods. *Thermochim Acta*. 1992;203:159–165.
8. Ozawa T. Thermal analysis-review and prospect. *Thermochim Acta*. 1999;355:35–42.
9. Augis JA, Bennett JE. Calculation of the Avrami parameters for heterogeneous solid-state reactions using a modification of the Kissinger method. *J Therm Anal*. 1978;13:283–292.
10. Lin CP, Chang YM, Tseng JM, Shu CM. Comparisons of nth order kinetic algorithms and kinetic model simulation on HMX by DSC tests. *J Therm Anal Calorim*. 2010;100:607–614.
11. Lin CP, Tseng JM, You ML, Chu YC, Shu CM. Modeling thermal decomposition kinetic algorithm on CL-20 and HMX. *Int J Chem React Eng*. 2010;8:A146.
12. Tsai LC, Wei JM, Chu YC, Chen WT, Tsai FC, Shu CM, Lin CP. RDX kinetic model evaluation by nth order kinetic algorithms and model simulations. *Adv Mater Res*. 2011;189–193:1413–1416.
13. Lin CP, Chang CP, Chou YC, Chu YC, Shu CM. Modeling solid thermal explosion containment on reactor HNIW and HMX. *J Hazard Mater*. 2010;176:549–558.
14. Lin CP, Tseng JM, Chang YM, Liu SH, Shu CM. Modeling liquid thermal explosion reactor containing tert–butyl peroxybenzoate. *J Therm Anal Calorim*. 2010;102:587–595.
15. Malow M, Michael-Schulz H, Wehrstedt KD. Evaluative comparison of two methods for SADT determination (UN H.1 and H.4). *J Loss Prev Process Ind*. 2010;26:740–744.
16. Bosch CM, Velo E, Recasens F. Safe storage temperature of peroxide initiators: prediction of self-accelerated decomposition temperature based on a runaway heuristics. *Chem Eng Sci*. 2001;56:1451–1457.
17. Fauske & Associates. *VSP2 Manual and Methodology*. Burr Ridge, IL: Fauske & Associates, 2003.

Manuscript received July 15, 2011, and revision received Dec. 22, 2011.